# Characteristics of underwater acoustic communication channels in shallow water

T.C. Yang
Naval Research Laboratory, Washington DC 20375

*Abstract* - **Underwater acoustic channels are band-limited and reverberant, posing many obstacles to reliable, phase-coherent acoustic communications. While many high frequency communication experiments have been conducted in shallow water, few have carried out systematic studies on the channel properties at a time scale relevant for communications. To aid the communication system design, this paper analyzes at-sea data collected in shallow water under various conditions to illustrate how the ocean environments (sea surface waves, and random ocean medium) can affect the signal properties. Channel properties studied include amplitude and phase variations, and temporal coherence of individual paths as well as the temporal and spatial coherence of multipaths at different time scales. Reasons for the coherence loss are hypothesized.**

## I. INTRODUCTION

Sound propagation in shallow water is heavily influenced by sound interactions with the inhomogeneities in the water column, and scattering from rough surfaces and bottom. Oceanographic processes in the water column include meso-scale and sub-meso-scale processes (e.g., front, offshore forcing, surface flux etc), (linear and non-linear) internal waves, fine-structure (spice/thermohaline) and micro-fine-structure (turbulence) inhomogeneities. These processes are different not only in spatial scale but also in time scale. The effects of these processes on underwater acoustic communications channels are not well understood. While many high frequency communication experiments have been conducted in shallow water, few have attempted to measure and characterize the channel systematically on the relevant scales [1]. Earlier works have reported the channel variations on the scale of tens of seconds to minutes [2,3]. In dynamic oceans (e.g., rough seas), the acoustic channel can vary on the scale of hundreds of milli-seconds or less. To determine whether a (particular) channel equalizer can cope with such variations, knowledge about channel variations (on the scale of channel coherence time ore less) will be needed [4,5] This paper addresses the channel variations by measuring channel impulse responses (CIRs) approximately every 0.12 seconds using communication data transmitted in packets. Temporal correlation between these CIRs reveals the channel variations within a packet, referred to as the *intra-packet* channel variations. From the measured CIRs, one can separate the multipaths into individual or groups of paths, and study the amplitude and phase variations and temporal correlation of these paths. The analysis is conducted for individual packets, since in many cases the channel has changed so much that the analysis across packets is meaningless.

The data were taken from experiments designed in a way such that the effects of the surface waves and ocean inhomogeneities on signal propagation can be largely separated to allow detailed analysis and theoretical interpretations. From the received data, CIR is estimated as a function of time and depth. The effect of the surface waves on the communication channel is illustrated in Sec. II. The effect of medium inhomogeneities on communication channel is illustrated in Sec. III. Section IV is a brief summary.

## II. INFLUENCE OF SURFACE WAVES

In an ocean with either a constant, or an upward refractive (winter) sound speed profile, or with a near-surface sound channel in which the source and/or receivers reside, signal interaction with the surface is unavoidable. To study the effect of rough surfaces on the communication channel, we analyze data from the 2007 Autonomous Underwater Vehicle Festival (AUVFest07) experiment conducted in

20 m of coast water under relatively calm and rough sea conditions, corresponding to sea states of 0 and 3 respectively (based on observed wave height and the presence and absence of white caps of breaking waves). The sound speed is nearly a constant for these environments. The source and receivers were deployed close to the bottom (1-2 m above the bottom) mounted on a rigid body so that signal fluctuation due to source or receiver motion is not an issue.

To study the channel temporal variations, we use binary phase shift keying (BPSK) signals employing a m-sequence code. An estimate of the CIR is obtained for each m-sequence (approximately every 0.1 sec) with little interference from the adjacent m-sequences due to the cyclic orthogonality of the m-sequence signal. One packet of ~25 sec duration provides ~200 independent estimates of the CIR as a function of time.

The measured CIRs are shown in Figs.1a and 2a for (relatively) calm and rough sea conditions. One finds that, when the sea surface is relatively smooth (calm sea), the multipaths have stable arrival times within the 25 sec. The dominant multipath arrivals show little fluctuation in amplitude mostly because they come in at shallow angles and are perhaps totally reflected by the sea surface. Some weak arrivals remain with a longer delay time; they fade in and out with time due to scattering from (small) sea surface waves.

When the sea surface is rough, one finds that all multipath arrivals are being affected by the sea surface. Even the dominant multipath arrivals show significant fading with respect to geotime (transmission) time, while showing stable arrival (delay) time. Many scattered later arrivals are evident in Fig. 2a.

1. Amplitude and Phase Fluctuation

Because the arrival (delay) times are stable, one can separate the dominant paths by time and study their amplitude and phase fluctuation. The separation is done as follows: one obtains an averaged intensity curve by averaging the intensities of all CIRs, from which one identifies the path arrival time, and their start and end time based on the intensity peaks and their -3 dB points. The start time and end time are used to gate (window) the time series for each path. Three paths are identified from Fig. 1a as indicated by the arrows below it, numbered 1, 2, and 3 from the left to the right. For each CIR, the amplitude of each path is obtained by the square root of the intensity integrated from the start time to the end time of each path. The histograms of the amplitudes are shown in Fig. 1b for the three paths, from which one can estimates the peak and the width (at -3 dB) of the distribution. One finds that the peak-to-width ratio is 21.1, 14.8, and 6.3 for the three paths. These ratios are much greater (by a factor of 3) than that expected for a Rayleigh distribution.

Similarly for the rough sea conditions, one identifies 5 dominant paths as shown by the arrows under Fig. 2a, numbered 1 to 5 from the left to the right. The amplitude histograms of individual paths are shown in Fig. 2b. One finds that the peak-to-width ratios are 4.2, 2.5, 2.8, 2.9 and 2.7 for path 1 to 5 respectively. In general, the higher the peak-to-width ratio the more deterministic the path is. The measured values are consistent with the fact that paths are less deterministic in rough than in calm sea conditions. (The above analysis is limited to data within one packet, since channels have changed significantly between packets under the rough sea conditions.)

The gated time series for each path, obtained from CIRs at different geotime times, are correlated to determine the temporal correlation of the corresponding path. One plots the maximum of the auto-correlation, normalized by the geometric mean of the path energies, as a function of the lag time between the CIRs as shown in Figs. 1c and 2c for the calm and rough sea conditions respectively. One finds that under the calm sea conditions, all three paths are consistently and highly coherent over the duration of the packet. Under the rough sea conditions the first 4 paths are highly coherent, except when they suffer from fading. The temporal coherence curves of path 3 and 4 are shown in Fig. 2c. Similar curves are found for path 1 and 2 but not shown. Temporal coherence for path 5 is somewhat lower than that for path 1 to 4 due to increased spreading and fading of the path as seen in Fig. 2a.

The phase of each path relative to its initial phase is determined from the phase of the path correlation. The results are shown in Figs. 1d and 2d for the calm and rough sea conditions. One finds that the phase changes relatively smoothly over time under calm sea conditions and more rapidly with time under the rough sea conditions (note the oscillations of the phase in Fig. 2d).

2. Intra-packet Temporal Coherence

While individual paths may remain temporally coherent, their combination may not, because the relative phases between them could vary rapidly with time. Multipath fluctuation can be measured in terms of the temporal coherence defined by [6]

$$\rho(\tau) \equiv \left\langle \frac{[p^*(t)p(t+\tau)]}{\sqrt{[p^*(t)p(t)][p^*(t+\tau)p(t+\tau)]}} \right\rangle, \quad (1)$$

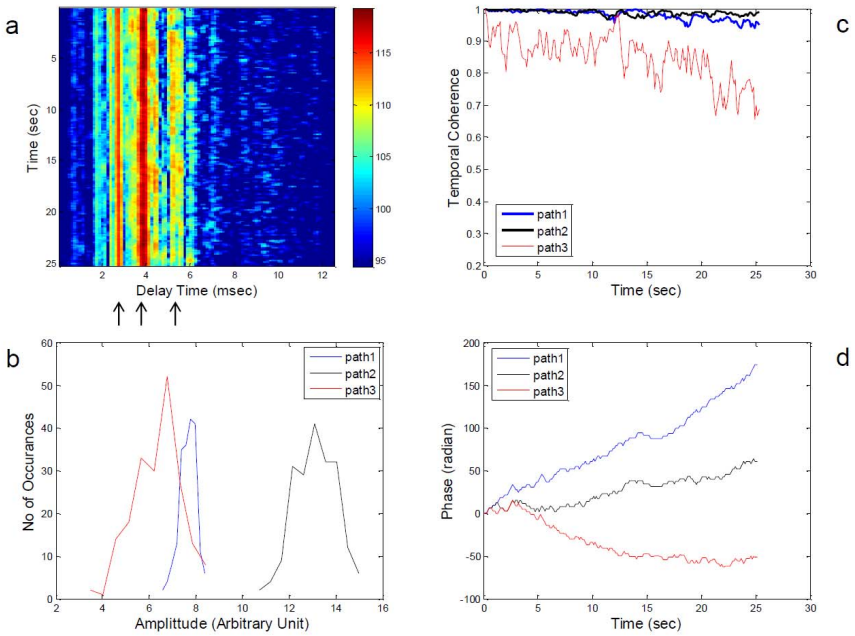


Fig. 1. (a) Measured CIRs under calm sea conditions. Color scale in dB. (b) Histogram of amplitude distributions for individual paths identified by arrows under Fig. 1a. (c) Temporal coherence of individual paths. (d) Phase variation of individual paths.

where $p(t)$ is the reference CIR at geotime $t$, and $p(t+\tau)$ is the CIR lagged by time $\tau$, the square bracket [a b] denotes the maximum value of the correlation between the a and b time series, and the <> bracket denotes ensemble average over the geotime $t$ (using reference signals transmitted at different geotimes).

Using the first CIR of each packet as the reference, averaging over many packets of data, the result is shown in Fig. 3a and 3b as a function of the lag time for the calm and rough sea conditions respectively. Noting that the CIRs are measured every ~0.1 s, the temporal coherence functions reported here reveal a "fast-time" variation of the channel as opposed to the "slow-time" variation of the channel across different packets, sampled every ~ 30 s (results not shown here).

One finds from Fig. 3 that the temporal coherence shows a high value (≥ 0.8) over 25 seconds under relatively calm sea conditions (Fig. 3a). In contrast, the temporal coherence under rough sea conditions drops to below 0.5 in a very short time (~0.2 seconds) (Fig. 3b). We observed above that even under the rough sea conditions, individual paths still maintain a high temporal coherence except when signal fades (Fig. 2c), but paths arrive with a rapidly varying phases. Hence, we attribute the loss of the multipath temporal coherence under rough sea conditions to both signal fading and rapidly varying (relative) phase between the dominant arrivals, as well as the increased presence of long diffused arrivals.

From Figs. 3a and 3b, one obtains an estimate of the coherence time, $\tau_{0.8}$, defined as the lag time when the coherence drops to 0.8. One finds that $\tau_{0.8}$ is approximately 0.1 s under rough-sea conditions during the AUVFest07 experiment (Fig. 3b). For the calm sea conditions, $\tau_{0.8}$ is about 30 sec (based on inter-

packet temporal correlation, results not shown here).

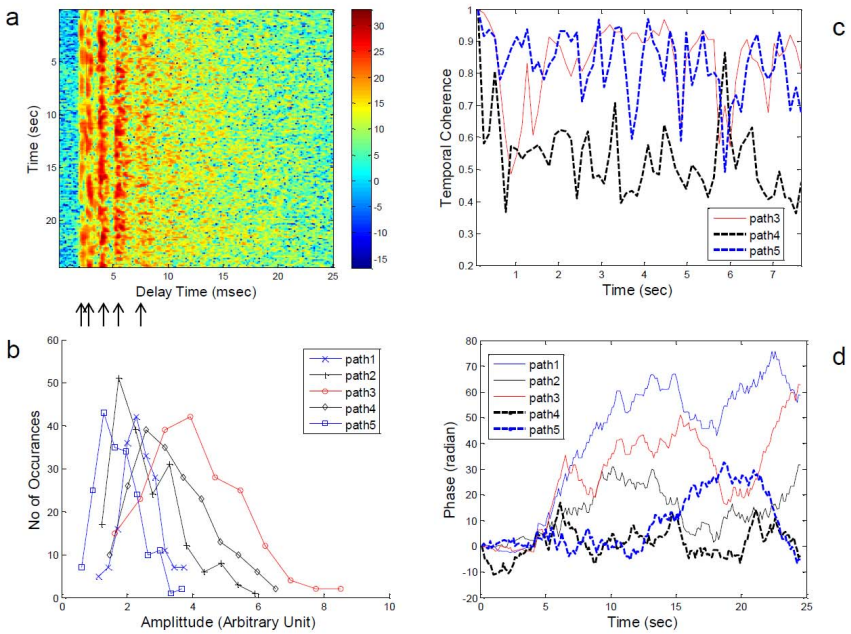


Fig. 2. (a) Measured CIRs under rough sea conditions. Color scale in dB. (b) Histogram of amplitude distributions for individual paths identified by arrows under Fig. 2a. (c) Temporal coherence of selected paths. (d) Phase variation of individual paths.

## III. INFLUENCE OF THE MEDIUM INHOMOGENEITIES

In other than winter time, the surface layer is usually warmer than water below, causing the sound to refract downward. The sound speed profile varies with range and time due to oceanographic processes created by the temperature/density differences inside the water column. To study the effect of random ocean medium on acoustic communications, we compare the open ocean data from the 2004 Time Reversal Experiment (TREX04) with data from the 2006 Underwater Network (UNet06) experiment, which was collected in a semi-stationary shallow water environment (protected bay). These two environments have approximately the same water depth, and a similar sound speed profile. The sea surfaces are relatively smooth. By placing the source and receivers below the thermocline, the effect of the surface waves on sound propagation can be "ignored" as most acoustic rays are refracted downward by the warm surface layer [7].

The TREX04 experiment took place on the New Jersey shelf (near the Mid-Atlantic Bight). Internal wave activities have been observed in this area during the summer time based on thermistor string data and high frequency backscattering images [8]. Turbulence can be generated by shear instability at the edge of internal waves. During the TREX04 experiments, no thermistor string was deployed, thus one cannot say positively whether internal waves were present. On the other hand, the SIMRAD backscattering sonar was deployed, which reveals abundant evidences of internal-wave like features from the backscattering images (in some areas more than others). The acoustic data analyzed below suggest that the signal encountered rapid temporal fluctuation, consistent with the hypothesis of a highly dynamic environment where internal waves and turbulences are a potential source contributing to the signal fluctuations.

Phase-shift keying signals were transmitted during these experiments with a carrier frequency centered at 17 kHz, with a bandwidth

of 4-5 kHz. To study the intra-packet channel variations, the data are segmented into blocks, each of ~0.1 sec long. The CIR is estimated for each block of data using the minimum mean square error (MMSE) channel estimation method. The data have high input signal-to-noise ratio (SNR) on the order of 20-25 dB. The method has been checked using m-sequence signals by comparing the results with that deduced using matched filter.

The measured CIRs are shown in Figs 4a and 5a using one packet of data from the UNet06 and TREX04 experiment. One notes that for the stationary environment (UNet06), the multipath delay times are quite stable within a packet. In contrast, for a dynamic ocean environment (TREX04), the multipath arrival times show variation with the measurement time due to channel variation with time. Some multipaths are found to split into micro paths. Many (weak) scattered arrivals are found following the main arrivals.

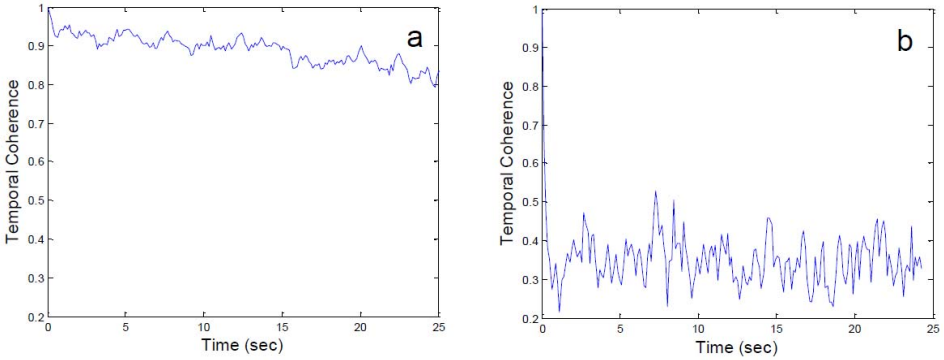


Fig. 3. Intra-packet temporal coherence as a function of lag time under calm sea (a) and rough sea conditions based AUVFest07 data.

1. Amplitude and Phase Fluctuation

Five paths are identified from Fig. 4a for the stationary ocean environment as indicated by the arrows below it. Their corresponding amplitude histograms are shown in Fig. 4b for the various paths. One notes that this is a minimum phase channel with the first path having significantly higher energy than the rest of the paths. However, even though the multipath arrival can be considered as almost deterministic, with stable arrival time, the energy of the first path varies over a much wider range that the other paths over the signal duration (~10 sec). This is shown by the histogram distribution of path 1 in Fig. 4b. The peak-to-width ratio is 4.6, 6.8, 4.6, 4.3, and 3.4 for path 1 to 5 respectively. Figure 4c shows that individual paths maintain a high temporal coherence over the packet length and Fig. 4d shows that paths have similar phases, with path 5 showing more phase fluctuations than the other paths.

For the open sea TREX04 environment, identification of individual paths is difficult because paths are split into micro-paths. We divide the dominant arrivals into three groups as indicated by the vertical bars under Fig. 5a. The later arrivals (following the dominant arrivals) are more difficult to characterize except to say that they are random in nature. For each CIR, one integrates the intensity of the CIR between the time separations (vertical bars) and takes the square-root to determine the amplitude for each group of paths. The histogram distributions of the amplitudes of the three groups of paths are shown in Fig. 5b. The histogram distribution of the No. 3 group suggests that group 3 is a combination of two subgroups each having a distribution similar to group 1 and 2. The temporal coherence curves of each group of arrivals are shown in Fig. 5c. One finds relatively high value of coherence (~ 0.7) for the three groups of paths despite the micro-path nature in each group of arrivals. The phases of each group of arrivals (each normalized by its initial phase) are shown in Fig. 5d as a function of transmission time. One finds that all three groups have similar phases for the first 6 seconds of data.

2. Intra-packet Temporal Coherence

The intra-packet temporal coherence is measured using Eq. (1), where $p(t)$ is the CIR measured from each block of data within each packet of data. Using the first CIR of each packet as the reference, and averaging over many packets of data, the result is shown in Fig. 6a and 6b as a function of the lag time for the UNet06 and TREX04 data. One finds that the temporal coherence of the intra-packet CIRs has a high value ($\geq 0.8$) over 10 seconds for the stationary UNet06 ocean environment (Fig.6a). In contrast, the intra-packet temporal coherence drops to below 0.6 in a very short time (~0.5 sec) for the open ocean TREX04 environment (Fig. 6b). Note that this temporal coherence calculation includes all paths. For the UNet06 data, one notes that despite the large amplitude variations of the first path, the signal remains highly coherent. This is attributed to the almost identical phases between the multipath arrivals. Note that multipath temporal coherence is more sensitive to the phase differences between the paths than the amplitude fluctuations of individual paths. In contrast, the TREX04 data also show high temporal coherence for individual groups of paths, and little phase differences between groups of arrivals (for the first 6 sec of data), yet the multipath coherence drops to below 0.5 in a short time. Observe from Fig. 5a, the split of arrivals into micro-paths and also the time-varying multipath arrival times. Thus, we attribute the loss of the intra-packet coherence (multipath coherence) in this case to the presence of micro-paths and time-varying multipath arrival times, as well as long diffused arrivals.

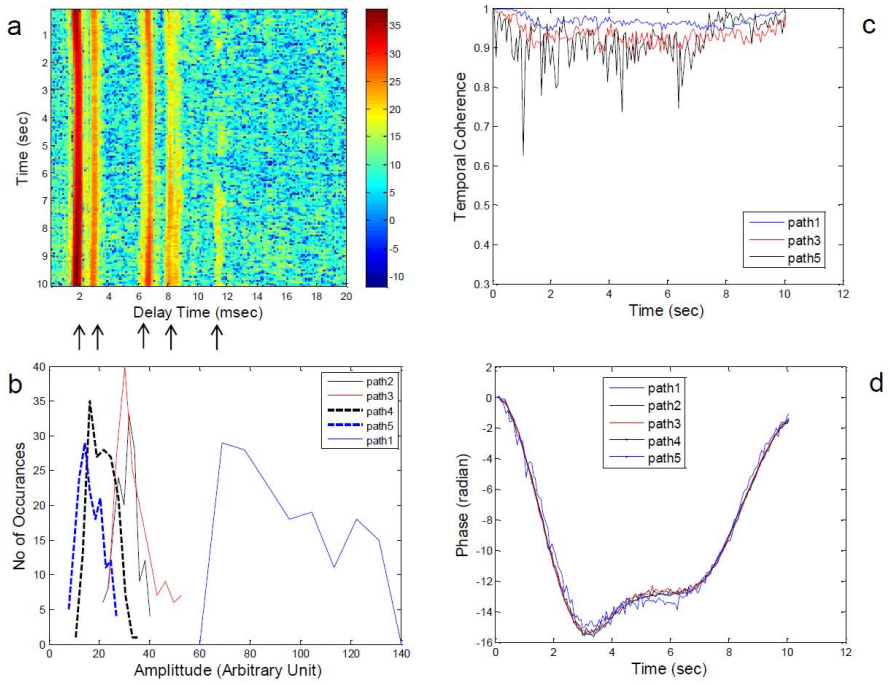


Fig. 4. (a) Measured CIRs from the UNet06 data. Color scale in dB. (b) Histogram of amplitude distributions for individual paths identified by arrows under Fig. 4a. (c) Temporal coherence of selected paths. (d) Phase variation of individual paths.

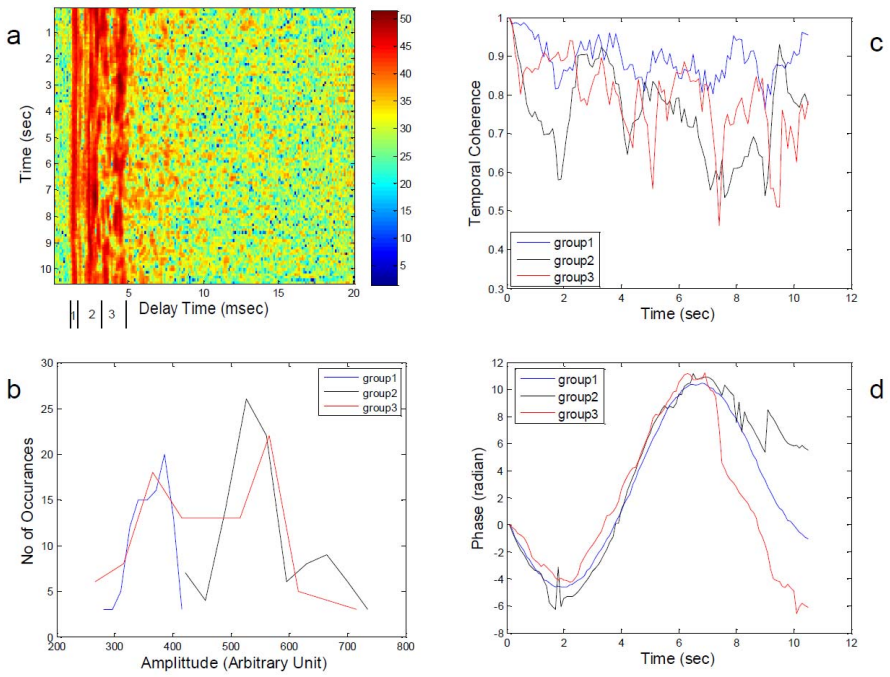


Fig. 5. (a) Measured CIRs from the TREX04 data. Color scale in dB. (b) Histogram of amplitude distributions for individual groups of paths delineated by vertical bars under Fig. 5a. (c) Temporal coherence of individual groups of paths. (d) Phase variation of individual groups of paths.

The temporal coherence time, $\tau_{0.8}$, is approximately 0.17 s based on TREX04 data (Fig.6b) and ~20 s for the UNet06 data based on temporal correlation of CIR between packets (result not shown here).

## IV. CONCLUDING REMARKS

This paper analyzes data from several recent experiments to illustrate the properties of underwater acoustic communication channels covering semi-stationary as well as dynamically changing environments. Data from 20 m of water with a constant sound speed profile are analyzed to study the effect of rough surface waves on high frequency communication channels. The effects of random oceanographic medium on communications are analyzed using data from protected to open ocean environments. In general, individual paths maintain high temporal coherence but the combination of them (the multipath coherence) may or may not, depending on the extent of surface roughness, and/or ocean inhomogeneities. Modeling the sound fluctuations through such complex environments remains very difficult at high frequencies due to limited knowledge of dynamics of the surface waves and fine/micro-fine structures at small spatial scales.

## ACKNOWLEDGEMENT

The work was supported by the Office of Naval Research.

1. D. B. Kilfoyle and A. B. Baggeroer, "The state of the art in underwater acoustic telemetry," IEEE J. Oceanic Eng., **25**, 4-27 (2000).
2. M.B. Porter, V.K. McDonald, P.A. Baxley, and J.A. Rice, "SignalEx: linking environmental acoustics with the signaling schemes," OCEANS 2000 MTS/IEEE Conference. Vol. 1, 595-600 (2000).
3. M. Siderius, M. B. Porter, P. Hursky, and V. McDonald, "Effects of ocean thermocline variability on noncoherent underwater acoustic communications," J. Acoust. Soc. Am. **121**, 1895 (2007).
4. A. Song, M. Badiey, H. C. Song, W. S. Hodgkiss, M. B. Porter, and the KauaiEx Group, "Impact of ocean variability on coherent underwater acoustic communications during the Kauai experiment (KauaiEx)," J. Acoust. Soc. Am. **123**, 856-865 (2008)

5. J. C. Preisig, "Performance analysis of adaptive equalization for coherent acoustic communications in the time-varying ocean environment," J. Acoust. Soc. Am., **118**, 263-278 (2005).
6. T. C. Yang, "Measurements of temporal coherence of sound transmissions through shallow water," J. Acoust. Soc. Am. **120**, 2595-2614 (2006).
7. M. B. Porter, S. M. Jesus, Y. Stephan, X. Demoulin and E. Coelho, "Tidal effects on source inversion," in *Experimental Acoustic Inversion Methods for Exploration of the Shallow Water Environment* edited by A. Caiti, J.-P. Hermand, S. M. Jesus and M. B. Porter, Kluwer Academic Publishers, 2000
8. J. Apel, et al., "An overview of the 1995 SWARM shallow water internal wave acoustic scattering experiment," IEEE J. Ocean. Eng. **22**, 465-500 (1997).

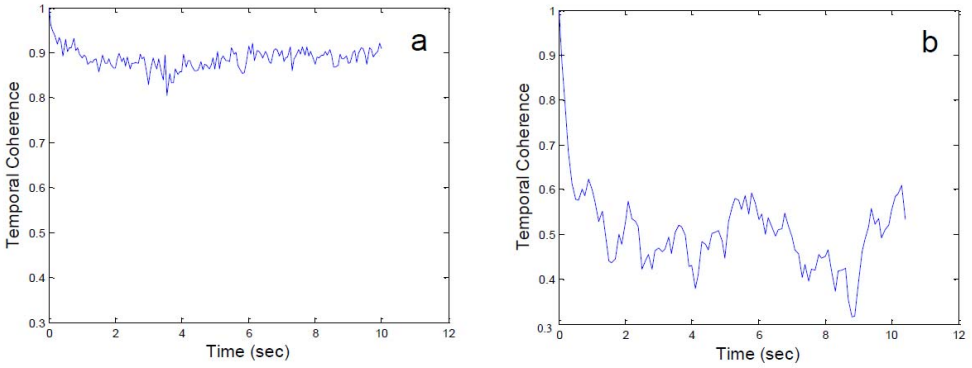


Fig. 6. Intra-packet temporal coherence as a function of lag time for the stationary ocean Unet06 (a) and open ocean TREX04 (b) environments.